Journal of Engineering, Project, and Production Management
2026, 16(4), 2025-274

Collaborative Control Strategy of Manufacturing Supply Chain Based on Multi-agent Swarm Intelligence Self-Organization

Hongmei Wang[1] and Guiping Zhao[2]
[1] Associate Professor, School of Business, Shandong Jianzhu University, Ji'nan, 250101, China,
[2] Lecturer, School of Civil Engineering, Shandong Polytechnic, Ji'nan, 250104, China, E-mail: zhaozgp0629@outlook.com (corresponding author)

Production Management
Received November 15, 2025; revised May 13, 2026; accepted May 13, 2026
Available online May 29, 2026

Abstract: This study proposes a self-organizing, collaborative control method for supply chains based on multi-agent swarm intelligence, incorporating consensus proactivity and cascading failure considerations. It aims to overcome the limitations of current supply chain control methods, such as poor real-time performance and high computational resource use. The research innovatively integrates carbon tax policies and time delay parameters to build a regulatory model that aligns with green development and practical communication constraints. It uses Karush-Kuhn-Tucker (KKT) conditions and the Lagrange multiplier method to ensure global optimality in convex optimization problems. A multi-agent self-organizing algorithm, grounded in consensus proactivity with a pheromone mechanism, is designed to improve system adaptability. Additionally, a cascading failure recovery strategy based on node importance is developed to increase supply chain resilience. Experiments demonstrate that transaction prices and volumes among different sellers tend to stabilize through iterations, confirming the effectiveness of multi-agent consensus control. The fastest convergence in average loss value is achieved by the consensus proactive method, reaching a minimum of 0.027. The central processor utilization rate, memory usage, and computation time are 26.2%, 173MB, and 25.3ms, respectively. In conclusion, the research effectively enhances supply chain response capabilities, improves regulation efficiency, and promotes sustainable development.

Keywords: Consensus initiative, cascading failure, multi-agent, swarm intelligence self-organization, supply chain regulation.

DOI 10.32738/JEPPM-2025-274

1. Introduction

With the rapid growth of the global economy, nations around the world have increasingly integrated their economies into an interconnected system across production, distribution, exchange, and consumption (Esmaeili et al., 2022; Meziani et al., 2023). While expanding manufacturing markets, economic globalization has also introduced characteristic challenges to supply chains, such as increased demand volatility, frequent node failures, and stricter environmental policies, such as carbon taxes (Thummalapeta and Liu, 2023). These factors collectively lead to a significant rise in supply chain complexity, which presents as non-linear and diverse traits (Ren et al., 2022; Gao et al., 2023). Traditional supply chain management methods are inadequate to address these dual aspects. Promoting intelligent and digital upgrades in supply chain management represents a new development direction for manufacturing supply chains (Nezamoddini and Gholami, 2022). To manage supply chain complexities within economic globalization, Sun et al. (2022) proposed a novel variable-order fractional supply chain network to handle uncertainties in supply-demand and delivery. This network employed Lyapunov exponents to analyze system dynamics and used a Chebyshev neural network estimator for multi-agent network control. Compared to integer-order models, it provides a more accurate depiction of complex system behavior. Experiments show that the system maintains stability under the Lyapunov stability theorem and Barbalat's lemma. Wang et al. (2022) introduced an adaptive protocol to solve the timing-coherent control problem in nonlinear multi-agent systems. This protocol employed adaptive update laws to enhance the model's capacity, and experiments confirmed that it effectively controlled the multi-agent system while reducing resource consumption within the intelligent agent system. Li and Zhou (2023) developed a swarm intelligence control method to address communication dependency issues in multi-agent control.

This approach used offline swarm learning, with each unit independently performing local frequency acquisition and integrating meta-reinforcement learning with evolutionary learning. Experimental results showed this method successfully reduced communication overhead while achieving optimal control. Shang et al. (2022) proposed a deep reinforcement learning control method for multi-agent energy-saving problems. This approach improved learning efficiency through multi-node parallel computation and used action representation techniques to address the high-dimensional nature of control problems. Experiments found that this method achieved maximum energy savings. In tackling green development challenges in supply chain collaborative regulation, Gupta et al. (2022) proposed a generalized game-theoretic model to examine how carbon emission sensitivity affects supply chains. This model considered decision-making paradigms based on collaboration and leadership within supply chains and represented uncertainties related to customer demand as fuzzy variables. However, when retailer demand uncertainty increased by 20%, the model showed that manufacturer profit fluctuations could reach ±15%, indicating limitations in its robustness.

In summary, existing research methodologies have explored issues such as supply chain collaborative regulation and green development from multiple perspectives, achieving certain results. However, limitations remain: most studies have not fully integrated green policy factors, such as carbon taxes, into real-time multi-agent collaborative regulation. Furthermore, traditional optimization algorithms often struggle to achieve real-time performance and consume excessive computational resources when addressing large-scale problems. Research into dynamic recovery mechanisms for supply chain cascade failures remains insufficient, necessitating a novel approach that simultaneously balances control efficiency, green constraints, and network resilience. Therefore, research has proposed a multi-agent SC regulation method based on consensus proactivity and cascading failures. This method innovatively introduces carbon tax policies and time-delay parameters, uses Karush-Kuhn-Tucker (KKT) conditions to ensure global optimality, employs centralized algorithms to solve the KKT conditions, utilizes consensus-based mechanisms and pheromones for multi-agent self-organizing regulation, and uses node importance for SC node fault recovery. The models and algorithms developed in this research specifically account for the characteristics of intelligent manufacturing environments. They simulate distributed decision-making units, such as smart warehouses and AGV scheduling, using multi-agent systems. The introduced time delay parameter aligns with the common asynchronous communication issues in industrial IoT, endowing the research methodology with inherent compatibility with Industry 4.0 environments centered on cyber-physical integration.

2. Methods and Materials

2.1. Optimal Control Strategy of Supply Chain (SC) Under Concept of Green Development

The concept of green development in the research is quantified by the carbon tax levied by the government, which occurs in the production process of manufacturer's products. Research constructs demand function models for manufacturers and sellers separately, where the cost function for manufacturers is given by Eq. (1) (Cao and Mei, 2022).

$$C_i(P_i) = a_i P_i^2 + b_i P_i + c_i \tag{1}$$

In Eq. (1), $C_i(P_i)$ represents the manufacturer's cost function, P_i represents the manufacturer's output, and a_i, b_i, and c_i respectively denote the manufacturer's fixed cost coefficient, linear variable cost coefficient, and quadratic variable cost coefficient. When all carbon taxes are paid by manufacturers, the social welfare function of manufacturers is calculated, as shown in Eq. (2) (Rezaei and Behnamian, 2022).

$$SW_{i,M}(P_i, Tp) = TpP_i - C_i(P_i) - ec_t P_i \tag{2}$$

In Eq. (2), $SW_{i,M}(P_i, Tp)$ represents the social welfare function of the manufacturer, Tp represents the price agreed upon between the manufacturer and the seller, e represents the carbon emissions per product of the manufacturer, and c_t represents the local carbon tax rate. The research assumes that the seller's sales volume is solely a function of price, and that the relationship between product price and sales volume is given by Eq. (3).

$$D(\tilde{p}) = d - \lambda \tilde{p} \tag{3}$$

In Eq. (3), $D(\tilde{p})$ represents the relationship function between product price and sales volume, $\tilde{p}$ represents the product sales price, d represents total sales volume, and λ represents the price sensitivity factor of consumers. The study selected a random number between the maximum and minimum delay values of two agents as the time delay, and the delay parameter between the two agents is calculated as shown in Eq. (4).

$$\begin{cases} \eta_{ij} = \left(\eta_{ij,\min}, \eta_{ij,\max}\right), i \neq j \\ \eta_{ij} = 0, i = j \end{cases} \tag{4}$$

In Eq. (4), η_{ij} represents the delay parameter between the intelligent agents i and j, $\eta_{ij,\min}$ denotes the mini delay value, and $\eta_{ij,\max}$ represents the max delay value. The study employs uniformly distributed simulated delays to preliminarily investigate the impact of communication asynchrony on collaborative control. This simplified model is widely used in the initial stages of theoretical analysis, with subsequent research to calibrate parameters based on empirically measured industrial IoT delay distributions (such as Poisson or Gamma distributions). The optimal control strategy objective function for the two-level Supply Chain (SC) of manufacturers and distributors is shown in Eq. (5).

$$\min_{P_i,D_j,Tp}\left(\sum_{i=1}^{m}\left(C_iP_i+ec_tP_i\right)-\sum_{j=1}^{n}U_jD_j\right) \tag{5}$$

In Eq. (5), U_j denotes the utility function of the j th seller, and D_j represents the product demand of the j th seller. This objective function aims to maximize the overall social welfare of the supply chain. The manufacturer's welfare function, defined by Eq. (2), incorporates both profits and carbon tax costs. The retailer's utility function U_j is typically related to sales revenue and market share and can be modeled as a concave function of product demand D_j. This reflects the economic principle of diminishing marginal utility, ensuring equilibrium between supply and demand. The optimization problem for the control strategy of a two-tier supply chain is a bicubic optimization problem. The function satisfies the properties of convexity within its domain and incorporates certain affine constraints. The objective function is formed by the sum of the manufacturer's concave welfare function and the distributor's concave utility function. Its Hessian matrix is negative definite, and the constraints are linear. Consequently, this problem represents a convex optimization problem, with the Karush-Kuhn-Tucker (KKT) conditions serving as both necessary and sufficient conditions for its global optimal solution. Therefore, the study uses KKT conditions to ensure the global optimality of the function, where $P_{i,\min}\le P_i\le P_{i,\max}$ and $D_{j,\min}\le D_j\le D_{j,\max}$ are and constraints. The Lagrange multiplier has clear economic significance, representing the shadow price associated with the constraint (such as a resource capacity constraint). It reflects the increase in the objective function value achievable by relaxing this constraint by one unit. The constructed Lagrangian function is denoted as $\iota\left(q,v,\varepsilon,\lambda\right)=\sum SW_{i,M}+\sum U_i+\varepsilon^T\eta\left(q,p\right)+\lambda^Th\left(q,p\right)$, where $\iota\left(\cdot\right)$ represents the Lagrangian function, T denotes transposition, ε and λ denote the Lagrangian multipliers corresponding to inequality constraints and equality constraints, respectively, $\eta\left(q,p\right)$ denotes the inequality constraints, and $h\left(q,p\right)$ denotes the equality constraints. The study used the Lagrangian method to decouple the objective function of the optimal regulation strategy and adopted a centralized algorithm to solve the KKT condition. The optimal production and purchase quantities of manufacturers and sellers were calculated, as shown in Eq. (6).

$$\begin{cases}P_i^c\left(k\right)=\dfrac{\kappa-b_i-ec_t}{2a_i}\\ D_j^c\left(k\right)=\dfrac{\beta_j-\kappa}{2\beta_j}\end{cases} \tag{6}$$

In Eq. (6), $P_i^c\left(k\right)$ represents the optimal production of the i th manufacturer, $D_j^c\left(k\right)$ denotes the optimal purchase quantity of the j th seller, k denotes the number of iterations, κ represents the marginal costs of the manufacturer and seller in the SC, and β_j represents the benefit function parameter of the j th consumer. The specific process of using centralized algorithms to solve KKT conditions is shown in Fig. 1.

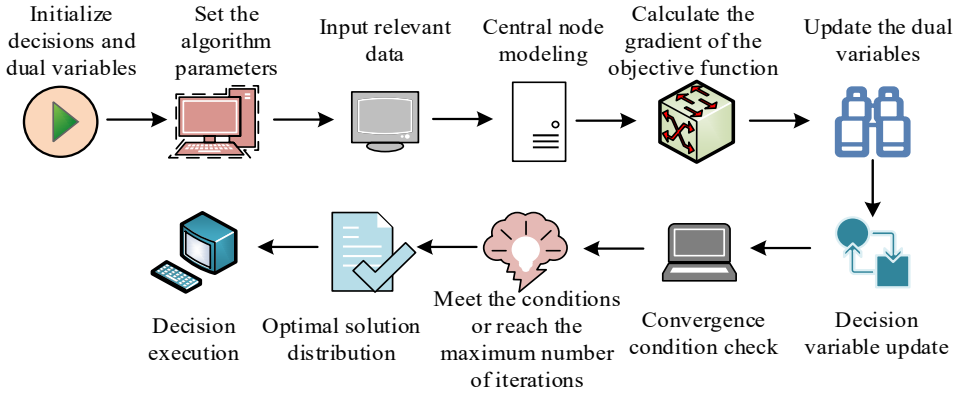

Fig. 1. Specific flow of the centralized algorithm to solve the KKT condition

In Fig. 1, the decision and dual variables are initialized, and the algorithm parameters, such as the step size and convergence threshold, are set. The objective function and constraint matrix data are input. Based on relevant data, a mathematical model is constructed at the central node, the gradient of the objective function is computed, and the dual and decision variables are updated in a timely manner. When all the convergence conditions are satisfied, or the maximum number of iterations is reached, the obtained solution and the dyadic variables are output, and the optimal solution is transmitted to the other participating nodes. In a multi-agent SC system, each agent's optimization objective is to coordinate product production and sales, as well as adjust product prices across regions. The unified consensus control protocol for multi-agent systems considering communication delay is denoted in Eq. (7) (Rashid et al., 2025).

$$\varepsilon_i(k+1)=\sum_{j\in V}x_{ij}\varepsilon_j\left(k-\eta_{ij}\right)+\mu\xi_i k \tag{7}$$

In Eq. (7), ε_i represents the multiplier corresponding to the i th inequality constraint in the Lagrange function, x_{ij} represents the relationship between the agents i and j, ε_j represents the multiplier corresponding to the j th inequality constraint, μ represents the iteration step size, and ξ_i represents the supply-demand mismatch variable.

2.2. Multi-Agent SC Collaborative Regulation based on Consensus Initiative

Although centralized SC regulation methods under the concept of green development can quickly reach global optimal solutions, in the multi-agent system of the SC, each agent faces a different environment, and the environment in which the agent operates is complex and constantly changing (Nozari, 2024). The consensus initiative mechanism is a coordination method used to describe biological populations and is widely applied in swarm intelligence and self-organizing behavior (Yin and Zhao, 2024). The multi-agent swarm intelligent self-organization mechanism using consensus initiative is shown in Fig. 2.

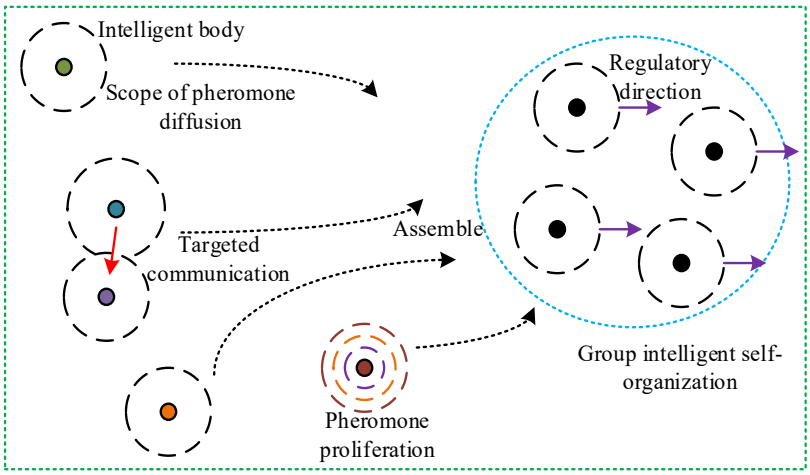

Fig. 2. Self-organization of multi-agent swarm intelligence based on consensus initiative

In Fig. 2, each agent can uniformly release pheromones in all directions, i.e., transmitting information. These pheromones carry the vendor's demand and pricing data, along with the manufacturer's inventory, production, quality, and logistics information. Parameters such as agent similarity are calculated, and agents with higher similarity are combined, while those with lower similarity are eliminated. Agent exploration state: Random movement with release of basic pheromones. Response state: calculating affinity upon detecting neighboring pheromone concentration exceeding a threshold. Cooperative state: establishing connections and adjusting self-state if affinity surpasses the threshold (seeking consensus and directing the release of response pheromones). Stable state: maintaining cooperative regulation within converged clusters until a task completion signal triggers dissolution. The specific process of the multi-agent self-organization algorithm based on consensus initiatives is shown in Fig. 3.

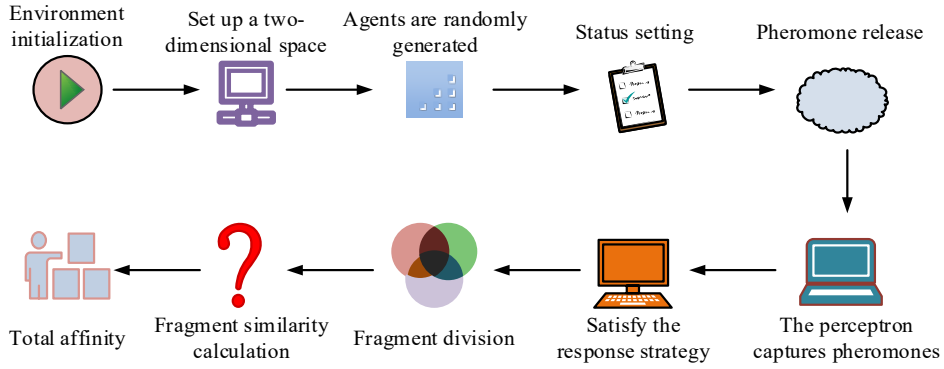

Fig. 3. Self-organization algorithm for multi-agent based on consensus initiative

In Fig. 3, environmental initialization is performed first, with coordinate points indicating the positions of individuals. Multiple agents are randomly generated and assigned corresponding states. The initial pheromone concentration of agents is set to zero and adjusted in real time based on task demand intensity. The generation and release of pheromones are triggered by each agent's real-time state. Individuals produce pheromones when seeking cooperation or when

environmental pressure rises. Adjacent agents detect nearby pheromone concentrations through sensors. When concentrations exceed preset thresholds, response logic is activated. Pheromone filtering involves segmenting information fragments, converting them into normalized vectors, calculating similarity using the Euclidean L2 norm, and then performing weighted computations. The L2 norm can simultaneously measure both the direction and magnitude differences between vectors, whereas cosine similarity is insensitive to magnitude, potentially resulting in high similarity scores between nodes with vastly different demand levels. The concentration calculation for uniform pheromone diffusion is shown in Eq. (8) (Jamalnia et al., 2023).

$$P_i(t,d_i^*)=\delta\frac{P_{max}^i(t)\cdot e^{-v/\tau}}{(\pi R_i)^{3/4}d_i^*} \tag{8}$$

In Eq. (8), $P_i(t,d_i^*)$ represents the pheromone diffusion concentration of the intelligent agent i, d_i^* represents the straight-line distance between the current calculation point and the agent releasing the pheromone, R_i represents the pheromone diffusion radius, v represents the lifetime of the pheromone, t represents time, and δ represents the correction coefficient. $P_{max}^i(t)$ represents the peak concentration at time t, $e^{-v/\tau}$ represents the pheromone decay factor, τ represents the time constant, and the pheromone concentration decays exponentially with time. The larger v or τ, the slower the decay. The total affinity calculation of each fragment of pheromone is shown in Eq. (9) (Leng et al., 2023).

$$S(A_i,A_k)=\sum_{j=1}^{n}\omega_j\cdot S \tag{9}$$

In Eq. (9), $S(A_i,A_k)$ represents the total affinity between agent i and agent k, A_i represents agent i, A_k represents agent k. n denotes the total number of segments of pheromones, ω_j represents the weight of segment j, and S represents the affinity of each segment. After all tasks in the SC are completed, each intelligent agent is restored to its initial state and waits for the next round of tasks.

2.3. SC Network Recovery based on Cascade Failure

Supply chain networks in the manufacturing sector face significant complexities, including high node loads, capacity imbalances, and external disturbances. These factors make supply chain networks more vulnerable to cascading failures, creating major challenges for their stable operation. Such failures can lead to higher economic costs, lower customer satisfaction, and damage to corporate reputation. Therefore, taking prompt recovery actions during cascading failures can effectively improve the supply chain's resilience against risks. When the overload state persists for too long, it may switch to a fault state. The state partitioning calculation for different intelligent agents is shown in Eq. (10) (Chamba et al 2023).

$$p_i(t)=\begin{cases}0, L_i(t)\le Q_i\\ 1, L_i(t)\ge(1+\varpi)Q_i\\ \dfrac{(1+\varpi)Q_i-L_i(t)}{\varpi Q_i}, Q_i<L_i(t)<(1+\varpi)Q_i\end{cases} \tag{10}$$

In Eq. (10), $p_i(t)$ represents the probability of the intelligent agent i being removed from the SC network, $L_i(t)$ represents the real-time load of the intelligent agent i, Q_i represents the capacity of the intelligent agent i, and ϖ represents the overload parameter of the intelligent agent. The safety factor may be established in accordance with the concept employed in systems engineering, with its value calibrated using historical data or system reliability requirements. When $p_i(t)$ is 1, the intelligent agent malfunctions and needs to be immediately removed from the SC network. When $p_i(t)$ is 0, it indicates that the intelligent agent is in a normal state and does not need to be removed. $Q_i<L_i(t)<(1+\varpi)Q_i$ indicates that the intelligent agent is in an overloaded state, with a removal probability between [0,1]. The removal of probability manifests at the system level. When the load of the failed node is successfully redistributed, and the load on all remaining nodes is less than or equal to the agent's capacity, the cascade failure process ceases, and the system enters a new stable state. The study performs SC network recovery based on node importance, structured as shown in Fig. 4.

In Fig. 4, fault recovery for supply chain nodes uses a randomized probability approach. When the random number surpasses the set recovery probability, the node is reactivated. Additionally, when two nodes in the supply chain are identical, they share the same recovery probability. To address variations in the supply chain network and the different criticality of nodes, research considers increasing the recovery probability for vital nodes. The more important a node, the higher its recovery probability. The study first ranks all nodes based on importance, as shown in Eq. (11) (Gherairi 2023).

$$A=\left\{A(i)\middle|1\le A(i)\le N\right\} \tag{11}$$

In Eq. (11), A represents the sorted set of importance levels for all nodes, $A(i)$ means the importance level of node

i, and N represents the total number of nodes in the SC. The study employs a multi-attribute comprehensive evaluation method to determine node importance, holistically considering degree centrality (measuring connection quantity), betweenness centrality (measuring network hub function), and betweenness-based load centrality (measuring traffic processing capacity). Each is assigned a normalized weight, with the sum of the three weights equaling one. Node importance is calculated as $A(i)=w_d \cdot DC(i)+w_b \cdot BC(i)+w_l \cdot LC(i)$, where w_d, w_b, and w_l denote the weight coefficients for degree centrality, betweenness centrality, and betweenness-based load centrality, respectively, while $DC(i)$, $BC(i)$, and $LC(i)$ represent the node's degree centrality, betweenness centrality, and betweenness-based load centrality, respectively. Subsequently, all nodes are ranked according to their importance values to yield the corresponding set. The recovery probability calculation of node i is shown in Eq. (12).

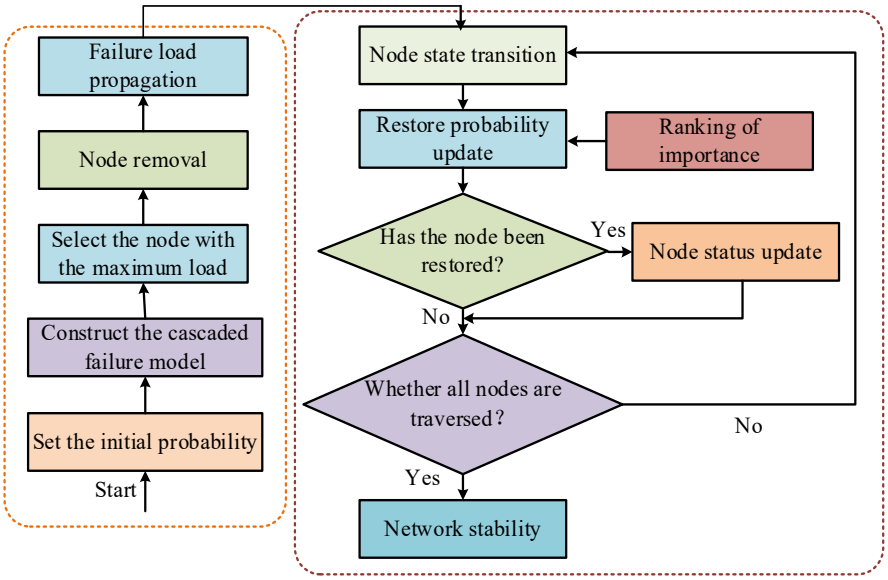

Fig. 4. SC network recovery based on node importance

$$Re(i)=\frac{A(i)}{\sum A(j)} \tag{12}$$

In Eq. (12), $Re(i)$ means the recovery probability of node i, and $\sum A(j)$ means the sum of all faulty nodes. The recovery probability of important nodes obtained from Eq. (12) is small, so reciprocal processing is required. The correct node recovery probability is shown in Eq. (13).

$$Re'(i)=\frac{1}{Re(j)\sum 1/Re(j)} \tag{13}$$

In Eq. (13), $Re'(i)$ represents the correct node recovery probability, and $Re(j)$ represents the sum of the recovery probabilities of all faulty nodes. Meanwhile, the study, to further improve the failure recovery efficiency of SC networks, passes the complexity of a node to the neighboring nodes. When the neighboring nodes are updated, and they can maintain the normal state, the load needs to satisfy Eq. (14).

$$Q_j < L_j(1) < (1+\varpi)Q_j \tag{14}$$

In Eq. (14), Q_j represents the capacity of adjacent node Q_j, and $L_j(1)$ represents the load of the adjacent node j. When adjacent nodes are updated, and in an overloaded state, the load satisfies Eq. (15).

$$L_j(1) > (1+\varpi)Q_j \tag{15}$$

The topology structure of the SC network is shown in Fig. 5.

In Fig. 5, before the cascading failure of the SC network, all nodes were connected to each other, and no isolated nodes appeared. After a cascading failure occurs, node X5 fails, and the X8 node connected to it also becomes isolated.

3. Results

3.1. Experimental Analysis of SC Regulation

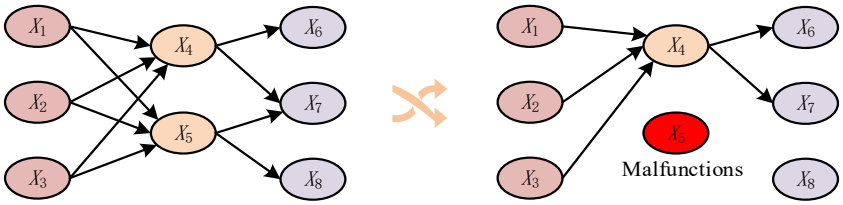

(a) Cascading Pre-Failure Supply Chain Networks

(b) Supply chain network after cascade failure

Fig. 5. Topology of the SC network

The study analyzed the proposed SC regulation method in simulation experiments. In the simulation experiment, the CPU was an Intel Core i5-12400 at 3.7 GHz, the GPU was an NVIDIA GeForce RTX 3080, and the memory was 32GB DDR5 at 3200 MHz. The software simulation environment operated on Python 3.9, incorporating the PyTorch framework for constructing multi-agent models. Simulation and interaction within the multi-agent system were implemented using the MASON library. The supply chain data originated from actual transaction records of a Chinese automotive components manufacturing enterprise spanning 2021 to 2023. The dataset comprised 12,450 transaction records involving 64 core enterprise nodes (including 3 manufacturers, 4 tier-one distributors, and numerous downstream distributors). When one of the manufacturers suddenly exited the SC, the changes in product transaction prices and delivery volumes in the SC are shown in Fig. 6.

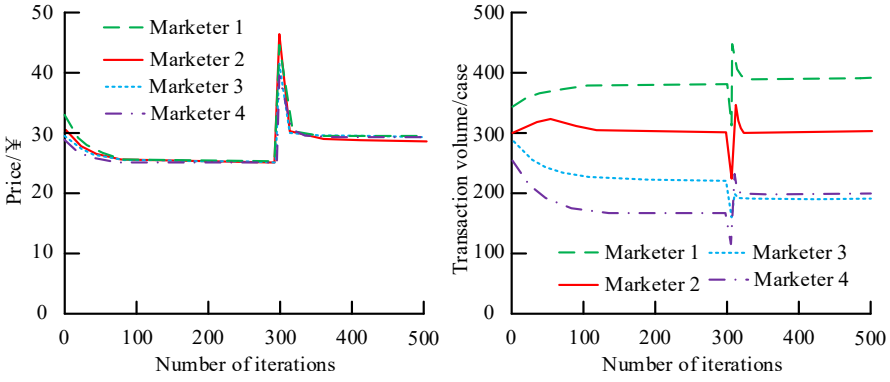

(a) Consistent transaction prices

(b) Volume of goods traded

Fig. 6. Changes in product transaction prices and deliveries in the SC

In Fig. 6(a), as the iteration progressed, the prices gradually converged. At 200 iterations, the transaction price converged to 26 yuan, and at 300 iterations, Marketer 2 withdrew from the SC, resulting in a sudden change in the transaction price, which then gradually converged to 29 yuan. In Fig. 6(b), after the exit of Marketer 2, the transaction volume of products for Marketers 1, 2, and 4 increased compared to before, while that of Marketer 3 decreased slightly. The withdrawal of manufacturers shifted the aggregate supply curve to the left. With demand remaining unchanged, the equilibrium price rose. The transaction volumes of Marketers 1, 2, and 4 increased, as they established closer synergies with the remaining Marketers 1 and 3, thereby securing reallocated production shares. Meanwhile, Marketer 3 experienced a slight decline in transaction volume because its product specifications were most closely aligned with Marketer 2's production capacity, leading to higher switching costs. The impact of different carbon tax quotas on the trading prices and delivery volumes of manufacturing products is shown in Fig. 7.

In Fig. 7(a), as the carbon tax rate progressively increased, the seller's transaction price gradually rose. When the carbon tax ranged from 0 to 0.4, the increase in transaction prices was modest. However, between 0.4 and 0.6, the rate of increase accelerated significantly. In Fig. 7(b), the decline in delivery volumes suddenly steepened once the carbon tax reached 0.4. At a carbon tax of 0.6, the delivery volumes for Marketers 1-4 were 182, 198, 205, and 179 boxes, respectively.

3.2. Experimental Analysis of Multi-Agent Self-Organization Regulation

The experimental hardware environment for multi-agent self-organizing regulation is identical to that described in Section 2.1. To thoroughly assess the performance of the proposed method, representative algorithms from self-organizing control and supply chain scheduling were chosen for comparison. The Particle Swarm Optimization Algorithm (PSO) is a well-known swarm intelligence optimization method; the Artificial Potential Field (APF) method is commonly used for real-time path planning and obstacle avoidance; the Distributed Control Law Method (DCLM) is a typical approach for distributed control; the Graph Theory-based Consensus Protocol (GTCP) serves as a benchmark for graph-theoretic consensus protocols, and Multi-Agent Reinforcement Learning (MARL) represents the cutting edge in multi-agent learning. These algorithms collectively cover different technical approaches for solving coordination problems across various domains. The average loss comparison of different self-organizing control methods in noisy environments is shown in Fig.

8.

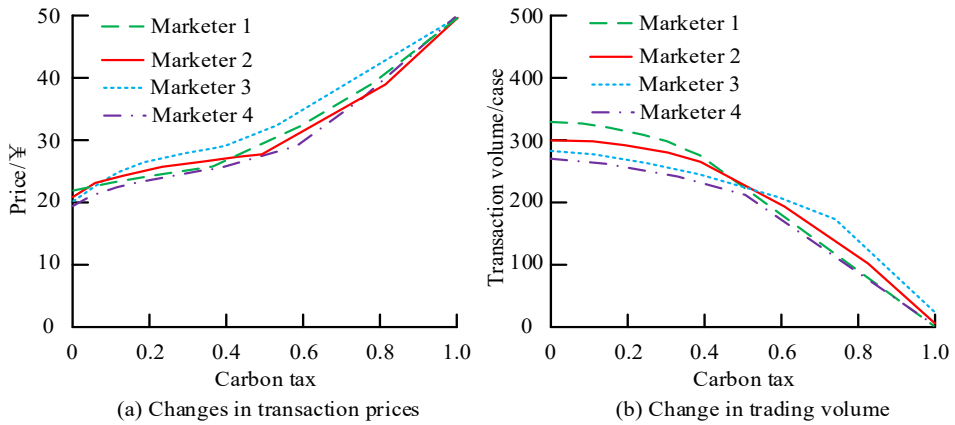

(a) Changes in transaction prices (b) Change in trading volume

Fig. 7. Impact of different carbon tax quotas on traded prices and deliveries of manufacturing products

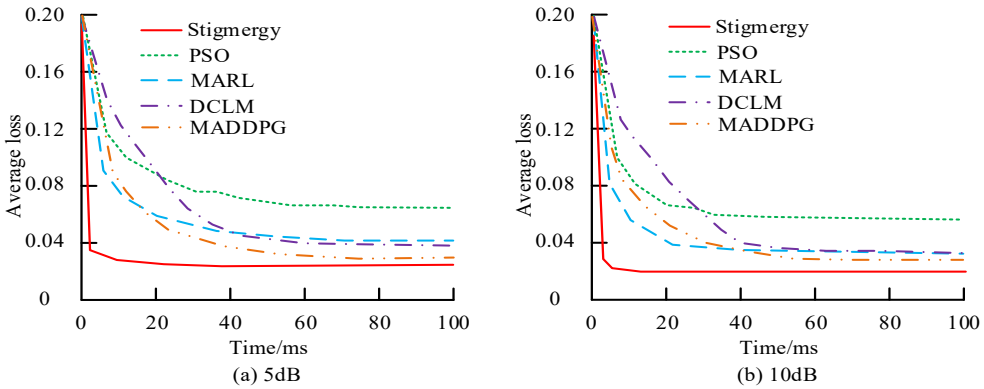

(a) 5dB (b) 10dB

Fig. 8. Comparison of average losses for different self-organized regulation methods

In Fig. 8 (a), all performance curves show the average results from 30 independent experiments. Statistical analysis of the final converged performance metrics was performed using t-tests, with a significance level of $p < 0.05$ for all four methods. The consensus-driven approach achieved a minimum mean loss of 0.027, which was 0.049, 0.024, 0.021, and 0.008 lower than the PSO, MARL, DCLM, and MADDPG methods, respectively. As shown in Fig. 8(b), the mean loss decreased for all methods as the signal-to-noise ratio increased, with the consensus-driven approach showing a reduction of 0.009 in the mean system loss. The comparison of root mean square errors (RMSEs) of intelligent agent states using different self-organization control methods is displayed in Fig. 9.

In Fig. 9 (a), the meaning was calculated after 30 independent experiments, with all methods showing a significance level of $p < 0.05$. The minimum RMSE of the consensus initiative method was 0.102, which was 0.115, 0.046, and 0.035 lower than the PSO, MARL, and DCLM methods, respectively. In Fig. 9 (b), the RMSEs of different methods all decreased. The RMSEs of the consensus initiative, PSO, MARL, and DCLM methods decreased by 0.017, 0.006, 0.04, and 0.005, respectively.

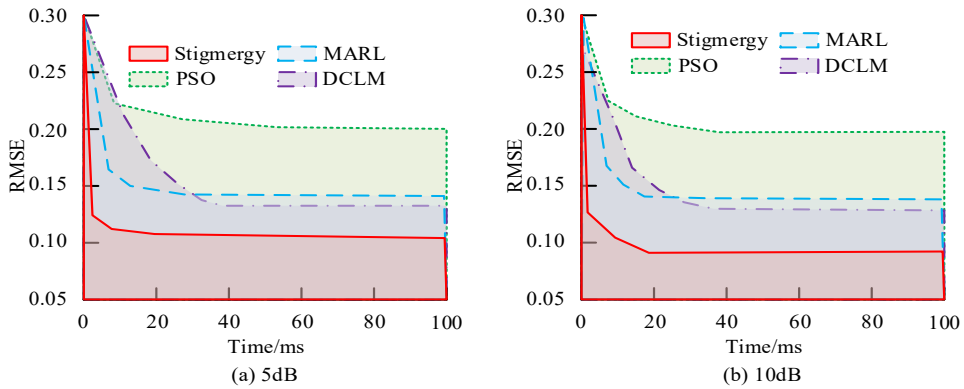

(a) 5dB (b) 10dB

Fig. 9. Comparison of RMSE of the states of intelligence with different self-organized regulation methods

3.3. Analysis of SC Network Recovery Experiment

The experiment set the initial load intensity of each node in the SC to 1.0, and the capacity and overload parameters of the nodes to 0.1. The study selected two SCs in the manufacturing industry, with a total of 64 and 92 nodes, respectively. The influence of different overload parameters on the proportion of failed nodes is shown in Fig. 10.

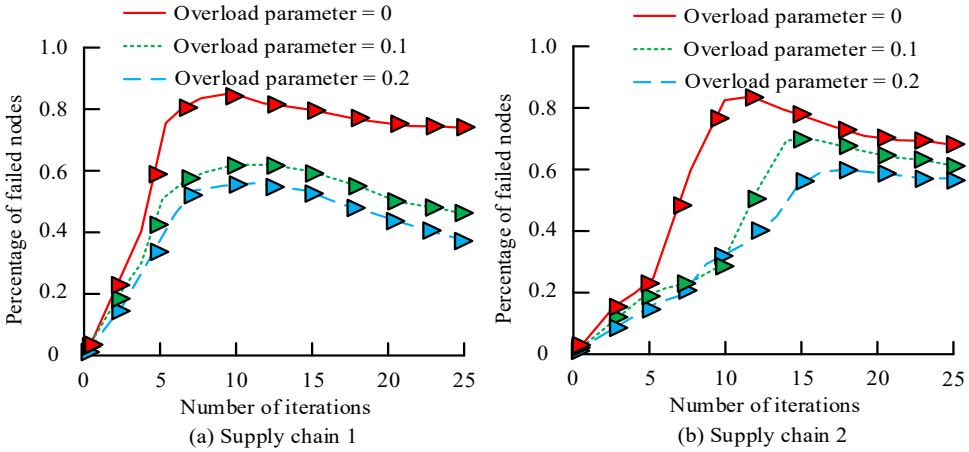

Fig. 10. Effect of different overload parameters on the proportion of failed nodes

In Fig. 10(a), as the overload parameter increased, the time for the failure node ratio to reach its maximum value became later, and the maximum failure ratio also decreased. When the overload parameter was 0, the maximum failure ratio was 0.85, which was 0.23 and 0.28 higher than when the overload parameter was 0.1 and 0.2, respectively. In Fig. 10(b), the failure rate of nodes decreased further, indicating that the larger the overload parameter, the slower the fault propagation speed in SC nodes, and the higher the node carrying capacity. The proportion of failed nodes in the SC network under different target recovery methods is shown in Table 1.

In Table 1, in SC 1, when the overload and capacity parameters were both 0.2, the failure node ratio of the importance recovery method was 0.51, which was 0.24, 0.22, and 0.23 lower than the equal probability recovery, degree objective recovery, and betweenness objective recovery, respectively. In SC 2, when the overload parameters were 0, 0.1, and 0.2, the proportion of failed nodes in the importance recovery method was 0.02, 0.12, and 0.13 lower than that of the second best method, respectively. The analysis of the impact of varying load fluctuation magnitudes on supply chain recovery is presented in Table 2.

In Table 2, as the load fluctuation amplitude increased from 0.1 to 0.5, the performance of all strategies declined. However, the performance degradation rate of importance-based recovery (from 8.2% to 29.3%) was significantly lower than that of the equal-probability recovery strategy (from 15.7% to 52.8%), indicating its superior adaptability to dynamic environments. The computational time for importance-based recovery consistently remained lower than that of equal-probability recovery.

4. Discussion

This study proposes a multi-agent supply chain regulation method based on consensus proactivity and cascading failures. Experiments demonstrate that when carbon taxes increase from zero to 0.6, transaction price rises exhibit nonlinearity, indicating the model's capacity to dynamically adjust supply and demand. Compared with the marginal cost allocation approach in Jamalnia et al. (2023), the welfare function introduced in this study more comprehensively reflects the social benefit losses incurred by manufacturers under carbon tax pressure. The L2-norm-based fragment similarity calculation filters out low-relevance information, reducing decision errors under noise interference and lowering the model's RMSE by over 35% compared to conventional methods. The proposed importance-weighted recovery strategy dynamically adjusts recovery probabilities, reducing the proportion of failed nodes in the supply chain by 24%. The load distribution mechanism prioritizes capacity-redundant nodes to assume failed loads, preventing secondary overloads.

This study also presents certain limitations. Whilst node importance assessment incorporates multiple metrics, complex dependencies may exist between nodes within intricate real-world supply chain networks. Moreover, the substantial initial deployment costs for both software and hardware hinder widespread adoption among small and medium-sized enterprises. Future research could introduce multi-layer network modeling to quantify the strength of causal dependencies between nodes, alongside the development of cloud-based, lightweight solutions to reduce initial investment burdens for SMEs.

5. Conclusion

To address the poor real-time performance of existing supply chain regulation methods, this study proposes a multi-agent swarm intelligence self-organizing supply chain regulation approach that leverages consensus proactivity and cascading failure. Experiments show that both transaction prices and volumes across different suppliers in the supply chain converge toward stability over time. The consensus proactivity approach demonstrates the fastest convergence rate for average loss

values, achieving a minimum average loss of 0.027-0.049, 0.024, and 0.021, respectively, lower than the PSO, MARL, and DCLM methods. A higher node capacity parameter is associated with a lower failure rate. When overparameterization is set to zero, the maximum failure ratio reaches 0.85, which is 0.23 and 0.28 higher than when overparameterization is set to 0.1 and 0.2, respectively. The proposed method can effectively regulate the supply chain network, reduce computational resource consumption, and accelerate regulation speed. Managers can dynamically adjust production and pricing when the carbon tax rate reaches a threshold (e.g., 0.4). By adopting a consensus-based coordination mechanism, average losses are reduced by up to 49%. At the same time, replacing the equal-probability recovery mechanism with a significance-weighted recovery mechanism reduces the number of failed nodes by 24%. Finally, given the method's low resource consumption, administrators can deploy it on edge devices. Consequently, supply chain control is shifting from centralized optimization toward self-organization. Administrators must embrace distributed intelligence rather than command-and-control models. Furthermore, carbon taxes are not linear costs but triggers for nonlinear market tipping points, prompting companies to adopt proactive rather than reactive green strategies.

Table 1. Proportion of failed nodes in SC network under different target recovery methods

Method	Proportion of failed nodes					
	Overload parameter = 0.2, SC 1			Capacity parameter = 0.2, SC 2		
	Volumetric parameter=0.05	Volumetric parameter=0.1	Volumetric parameter=0.2	Overload parameters=0	Overload parameters=0.1	Overload parameters=0.2
Equal probability recovery	0.95	0.87	0.75	0.96	0.85	0.81
Degree target recovery	0.88	0.80	0.73	0.87	0.74	0.70
Median target recovery	0.92	0.85	0.74	0.91	0.79	0.75
Importance Recovery	0.84	0.62	0.51	0.85	0.62	0.57

Table 2. Impact of different load fluctuation magnitudes on supply chain recovery

Amplitude of fluctuation	Recovery Strategy	Performance degradation rate (%)	Recovery time increase (%)	Stability retention rate (%)
0.1	Importance Recovery	8.2	12.5	91.8
	Equal probability recovery	15.7	28.3	84.3
0.3	Importance Recovery	18.7	31.2	81.3
	Equal probability recovery	34.5	62.1	65.5
0.5	Importance Recovery	29.3	48.7	70.7
	Equal probability recovery	52.8	95.4	47.2

Author Contributions

Hongmei Wang contributed to methodology, data collection, draft preparation, and manuscript editing. Guiping Zhao contributed to methodology, analysis, investigation, manuscript editing, visualization, and supervision.

Funding

This research received no specific financial support from any funding agency.

Institutional Review Board Statement

Not applicable.

Declaration of Artificial Intelligence (AI) Tools

The authors used DeepSeek solely for language editing and readability improvement. The authors reviewed and verified all content and take full responsibility for the accuracy and integrity of the manuscript.

References

Cao, K., and Mei, Y. (2022). Green supply chain decision and management under manufacturer's fairness concern and risk aversion. *Sustainability*, 14(23), 16006-16039. doi: 10.3390/su142316006.

Chamba, A., Barrera-Singaña, C., and Arcos, H. (2023). Optimal reactive power dispatch in electric transmission systems using the multi-agent model with volt-VAR control. *Energies*, 16(13), 5004-5037. doi: 10.3390/en16135004.

Esmaeili Avval, A., Dehghanian, F., and Pirayesh, M. (2022). Auction design for the allocation of carbon emission allowances to supply chains via multi-agent-based model and Q-learning. *Computers and Applied Mathematics*, 41(4), 170-192. doi: 10.1007/s40314-022-01868-5.

Gao, J., Zhang, W., Guan, T., and Feng, Q. (2023). Evolutionary game study on multi-agent collaboration of digital transformation in service-oriented manufacturing value chain. *Electronic Commerce Research*, 23(4), 2217-2238. doi: 10.1007/s10660-022-09532-0.

Gherairi, S. (2023). Design and implementation of an intelligent energy management system for smart home utilizing a multi-agent system. *Ain Shams Engineering Journal*, 14(3), 101897-101925. doi: 10.1109/isgt-asia.2015.7386985.

Gupta, R., Goswami, M., Daultani, Y., Biswas, B., and Allada, V. (2023). Profitability and pricing decision-making structures in presence of uncertain demand and green technology investment for a three tier supply chain. *Computers & Industrial Engineering*, 179(6), 109190-109214. doi: 10.1016/j.cie.2023.109190.

Jamalnia, A., Gong, Y., Govindan, K., Bourlakis, M., and Mangla, S. K. (2023). A decision support system for selection and risk management of sustainability governance approaches in multi-tier supply chain. *International Journal of Production Economics*, 6(26), 108960-108993. doi: 10.1016/j.ijpe.2023.108960.

Leng, J., Sha, W., Lin, Z., Xing, J., Liu, Q., and Chen, X. (2023). Blockchained smart contract pyramid-driven multi-agent autonomous process control for resilient individualised manufacturing towards Industry 5.0. *International Journal of Production Research*, 61(13), 4302-4321. doi: 10.1080/00207543.2022.2089929.

Li, J., and Zhou, T. (2023). Evolutionary multi-agent deep meta reinforcement learning method for swarm intelligence energy management of isolated multi-area microgrid with internet of things. *IEEE Internet of Things Journal*, 10(14), 12923-12937. doi: 10.1109/jiot.2023.3253693.

Meziani, A., Bourouis, A., and Chebout, M. S. (2023). NeutroMAS4SCRM: A combined multi-agent system with neutrosophic data analytic hierarchy process framework for supply chain risk management. *Journal of Intelligent & Fuzzy Systems*, 44(3), 3695-3716. doi: 10.3233/jifs-222305.

Nezamoddini, N., and Gholami, A. (2022). A survey of adaptive multi-agent networks and their applications in smart cities. *Smart Cities*, 5(1), 318-347. doi: 10.3390/smartcities5010019.

Nozari, H. (2024). Green Supply Chain Management based on Artificial Intelligence of Everything. *Journal of Economics and Management*, 46, 171-188. doi: 10.22367/jem.2024.46.07.

Rashid, A., Baloch, N., Rasheed, R., and Ngah, A. H. (2025). Big data analytics-artificial intelligence and sustainable performance through green supply chain practices in manufacturing firms of a develope country. *Journal of Science and Technology Policy Management*, 16(1), 42-67. doi: 10.1108/jstpm-04-2023-0050.

Ren, L., Fan, X., Cui, J., Shen, Z., Lv, Y., and Xiong, G. (2022). A multi-agent reinforcement learning method with route recorders for vehicle routing in supply chain management. *IEEE Transactions on Intelligent Transportation Systems*, 23(9), 16410-16420. doi: 10.1109/tits.2022.3150151.

Rezaei, S., and Behnamian, J. (2022). A strategic scheme for partnership supply networks focusing on green multi-agent transportations: A game theory approach. *Environmental Science and Pollution Research*, 29(54), 81830-81863. doi: 10.1007/s11356-022-21282-y.

Shang, M., Zhou, Y., Mei, Y., Zhao, J., and Fujita, H. (2022). Energy-saving train operation synergy based on multi-agent deep reinforcement learning on spark cloud. *IEEE Transactions on Vehicular Technology*, 72(1), 214-226. doi: 10.1109/tvt.2022.3205379.

Sun, T. C., Yousefpour, A., Karaca, Y., Alassafi, M. O., Ahmad, A. M., and Li, Y. M. (2022). Dynamical investigation and distributed consensus tracking control of a variable-order fractional supply chain network using a multi-agent neural network-based control method. *Fractals*, 30(5), 2240168. doi: 10.1142/s0218348x22401685.

Thummalapeta, M., and Liu, Y. C. (2023). Survey of containment control in multi-agent systems: Concepts, communication, dynamics, and controller design. *International Journal of Systems Science*, 54(14), 2809-2835. doi: 10.1080/00207721.2023.2250041.

Wang, L., Zou, M., Guo, W., Alsubaie, H., Alotaibi, A., Taie, R. O. A., and Jahanshahi, H. (2022). Adaptive discontinuous control for fixed-time consensus of nonlinear multi-agent systems. *Electronics*, 11(21), 3545-3567. doi: 10.2139/ssrn.4715287.

Yin, S., and Zhao, Y. (2024). An agent-based evolutionary system model of the transformation from building material industry (BMI) to green intelligent BMI under supply chain management. *Humanities and Social Sciences Communications*, 11(1), 1-15. doi: 10.1057/s41599-024-02988-5.

Hongmei Wang, born in October 1980 in Qingdao, Shandong Province, is a Han Chinese descendant. She earned her bachelor's degree in Engineering Management from Shandong Institute of Architectural Engineering in 2003, followed by a master's degree in Technology Economics and Management from Shandong University in 2006. In 2020, she completed her doctoral studies in Agricultural Economic Management at Shandong Agricultural University. Her research focuses on organizational and management systems in the agricultural and forestry industries. From 2006 to the present, she has been a full-time teacher and associate professor in the Business School of Shandong Jianzhu University. She has published four academic papers, one monograph and has been in charge of or participated in eight research projects.

Guiping Zhao was born in June 1979. She is of Han nationality, and her ancestral home is Rizhao City, Shandong Province. She graduated from Qingdao Institute of Architecture and Engineering with a bachelor's degree in Engineering Management in 2003. In 2006, she obtained a master's degree in Technology Economics and Management from Shandong University. Since 2006, she has been working as a full-time teacher and lecturer at Shandong Polytechnic. She has published two academic papers and presided over or participated in four teaching and scientific research projects.